## Supplemental Figures and Tables Summary

Figure S1 shows a lack of apoptosis by several methods: western blots detecting cleaved-Caspase 3 and cleaved-PARP, and TUNEL staining for nicked DNA. Figure S2 shows representative gene clusters from DAVID analysis of genes down-regulated in KD-VEGF (blood vessel, Golgi) as well as a "Foxo1 target" cluster assembled from the literature. Figure S3 shows microarray validation and changes in Foxo1 target genes in KD-VEGF conditions by RT-PCR. Figure S4 investigates possible upstream signaling pathways that may contribute to Foxo1 stability. Table S1 and S2 provide a detailed list of the top ontological clusters derived from the list of genes most changed between KD-VEGF and KD-NT HUVECs in an RNA microarray. Table S3 and S4 provide the top clusters derived from the list of genes responding to Foxo1 rescue following "Expression Pattern 1" (Table S3) and "Expression Pattern 2" (Table S4).

**Supplemental Figure 1.** Apoptosis was not detected in KD-VEGF HUVECs. (A) Total and cleaved Caspase 3 were detected by western blot in 25ug of protein lysate from KD-VEGF and KD-NT HUVECs. (B) Total and cleaved PARP were analyzed as above. Positive and negative apoptosis controls were provided by non-treated and staurosporine (1hr 1μM) treated HUVECs. (C) TUNEL staining was performed on KD-VEGF and KD-NT cells. Out of approximately 50,000 cells, 4 were found to be TUNEL positive in the KD-VEGF condition, while none were TUNEL positive in KD-NT. Nuclease treatment was used to create nicked DNA as a positive control. Error bars mean +/- SD, *, $P<0.05$; **, $P<0.005$

**Supplemental Figure 2.** Autocrine VEGF is required to maintain endothelial identity, mitochondrial and Golgi transcriptome. HUVECs were transfected with siRNA targeting VEGF and total RNA was isolated on day 4 after first transfection (n=3). Gene expression profile was assessed with Illumina human gene chip expression assay. GO clusters extracted from genes significantly up- and down-regulated in KD-VEGF analyzed by DAVID. Heatmaps highlight a subset of two down-regulated GO clusters: (A) blood vessel and (B) Golgi. (C) Select Foxo1 targets significantly up- or down-regulated.

**Supplemental Figure 3.** Microarray validation and further analysis of Foxo1 target genes (A) A significant decrease in VEGF levels was maintained in double-knockdown conditions. Two of the top genes found (B) increased (CCL23 and NDRG4) and (C) decreased (ESM1 and TAGLN) in the KD-VEGF condition of the microarray were validated by RT-PCR. (D) RT-PCR analysis of several genes of interest showed that decrease in VEGF levels was maintained over several days, Foxo1 levels remained largely unchanged, and VEGFR-2 levels were drastically increased. Several previously-described Foxo1 targets were found to be (E) increased as expected in the KD-VEGF condition by RT-PCR (CITED2, SOD2, SEPP1) or (F) found to be unchanged or regulated contrary to previous reports (SPRY2, MMP7, DCN, ID2, CCND1, CCNB2). Error bars mean +/- SD, *, $P<0.05$; **, $P<0.005$

**Supplemental Figure 4.** No changes observed in signaling pathways upstream of Foxo1 or in phospho-Foxo1 levels. Western blots investigating the phospo- activation status of (A) Akt, (B) JNK and (C) AMPK were performed, revealing no significant differences between KD-VEGF and KD-NT conditions. (D) Western blots were performed and quantified showing phospho-Foxo1 status was unchanged relative to total Foxo1 protein in KD-NT and KD-VEGF HUVECs.

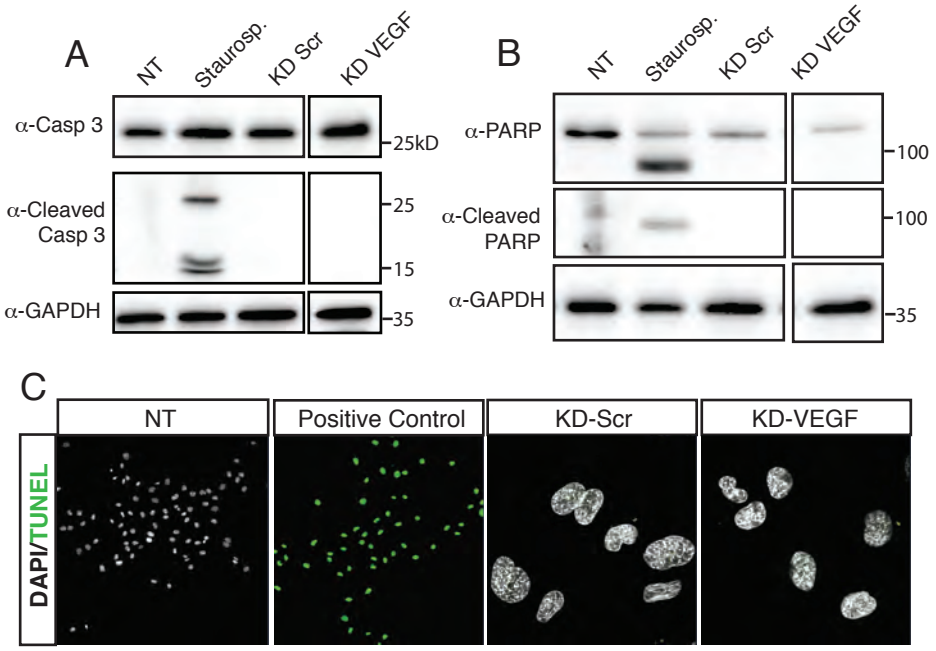


**Supplemental Figure 1: Apoptosis was not detected in KD-VEGF HUVECs**

(A) Total and cleaved Caspase 3 were detected by western blot in 25ug of protein lysate from KD-VEGF and KD-Scr HUVECs. (B) Total and cleaved PARP were analyzed as above. Positive and negative apoptosis controls were provided by non-treated and staurosporine (1hr 1uM) treated HUVECs. (C) TUNEL staining was performed on KD-VEGF and KD-Scr cells. Out of approximately 50,000 cells, 4 were found to be TUNEL positive in the KD-VEGF condition, while none were TUNEL positive in KD-Scr. Nuclease treatment was used to create nicked DNA as a positive control.

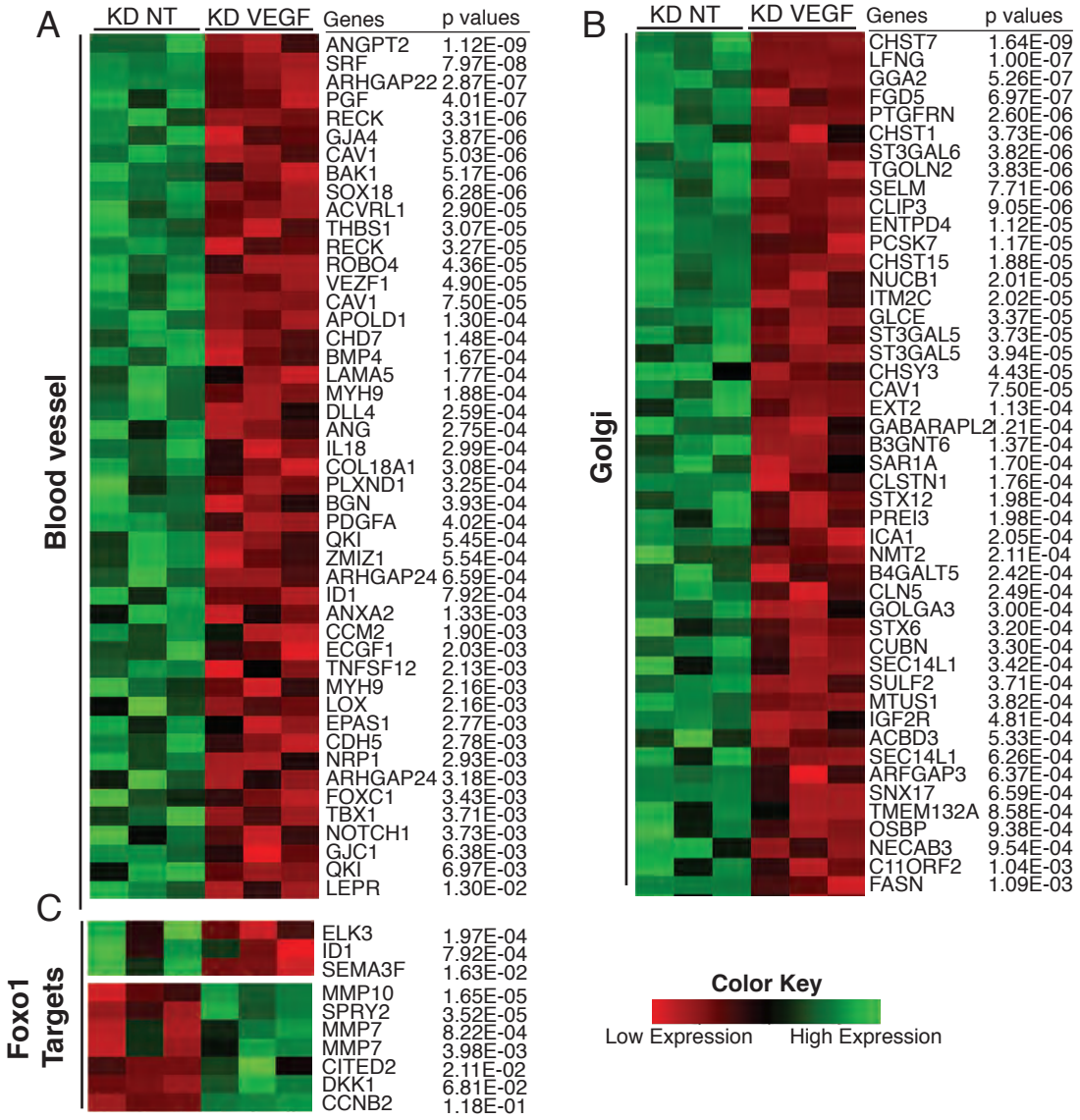


**Supplemental Figure 2: Autocrine VEGF is required to maintain endothelial identity, mitochondrial and Golgi transcriptome**

**HUVECs were transfected with siRNA t**argeting VEGF and total RNA was isolated on day 4 after first transfection (n=3). Gene expression profile was assessed with Illumina human gene chip expression assay. GO clusters extracted from genes significantly up- and down-regulated in KD-VEGF analyzed by DAVID. Heatmaps highlight a subset of two down-regulated GO clusters: (A) blood vessel and (B) Golgi. (C) Select Foxo1 targets significantly up- or down-regulated.

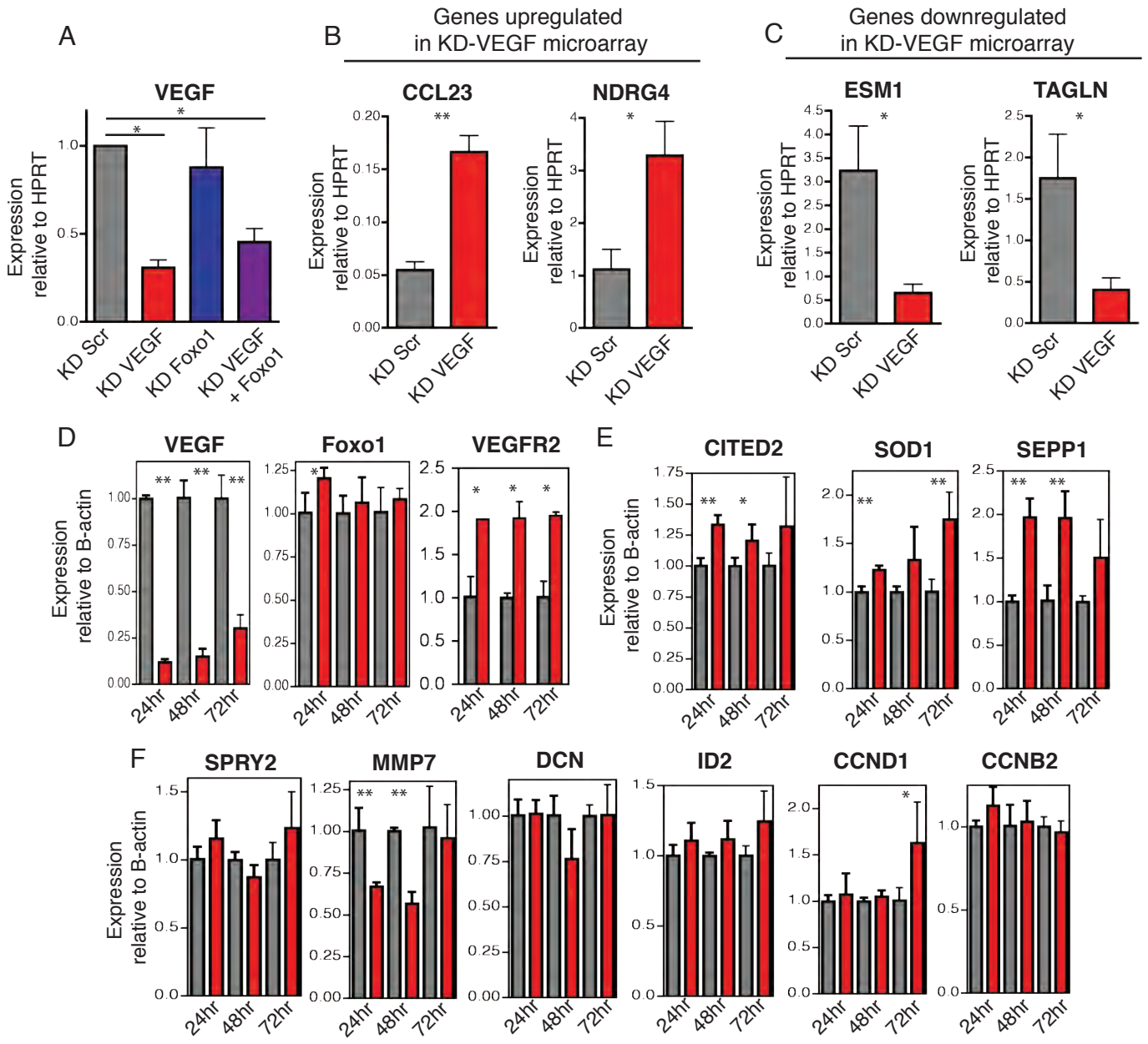


**Supplemental Figure 3: Microarray validation and further analysis of Foxo1 target genes**

(A) A significant decrease in VEGF levels was maintained in double-knockdown conditions. Two of the top genes found (B) increased (CCL23 and NDRG4) and (C) decreased (ESM1 and TAGLN) in the KD-VEGF condition of the microarray were validated by RT-PCR. (D) RT-PCR analysis of several genes of interest showed that decrease in VEGF levels was maintained over several days, Foxo1 levels remained largely unchanged, and VEGFR-2 levels were drastically increased. Several previously-described Foxo1 targets were found to be (E) increased as expected in the KD-VEGF condition by RT-PCR (CITED2, SOD2, SEPP1) or (F) found to be unchanged or regulated contrary to previous reports (SPRY2, MMP7, DCN, ID2, CCND1, CCNB2).

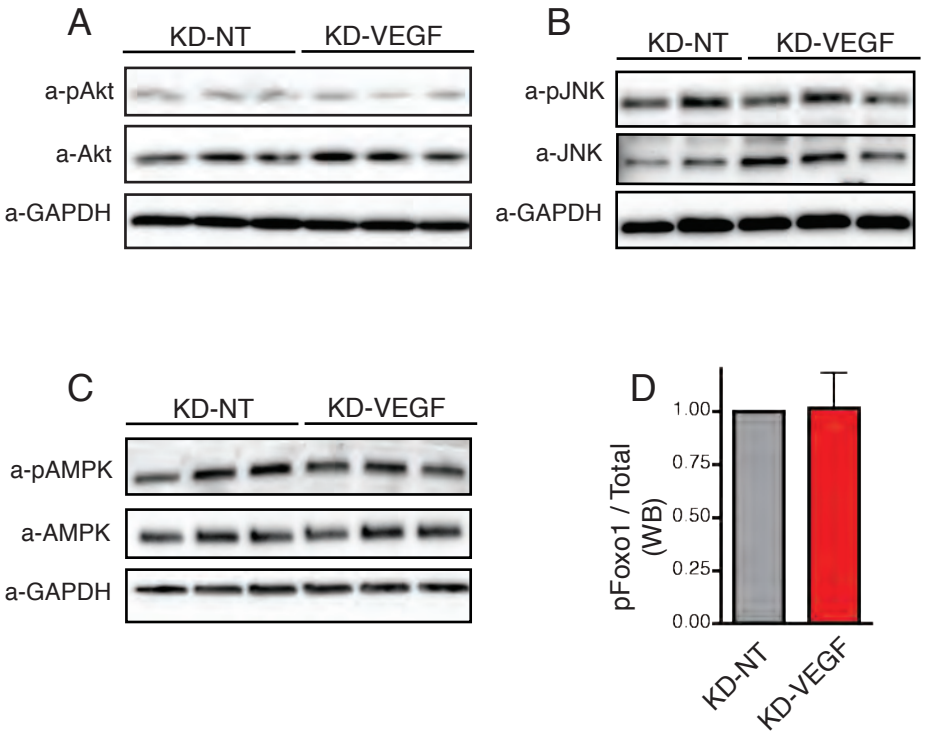


**Supplemental Figure 4.** No changes observed in signaling pathways upstream of Foxo1 or in phospho-Foxo1 levels. Western blots investigating the phospo- activation status of (A) Akt, (B) JNK and (C) AMPK were performed, revealing no significant differences between KD-VEGF and KD-NT conditions. (D) Western blots were performed and quantified showing phospho-Foxo1 status was unchanged relative to total Foxo1 protein in KD-NT and KD-VEGF HUVECs.

**Table S1 – DAVID analysis of genes significantly downregulated in KD-VEGF**

| GO Cluster | Term | Count | Benjamini | Fold Enrichment |
|---|---|---|---|---|
| **Cluster 1 – Enrichment Score: 9.02** | | | | |
| | Golgi apparatus | 128 | 8.53E-09 | 1.78 |
| | GO:0005794-Golgi apparatus | 175 | 4.96E-07 | 1.54 |
| | GO:0044431-Golgi apparatus part | 75 | 1.88E-06 | 1.96 |
| **Cluster 2 – Enrichment Score: 6.88** | | | | |
| | GO:0001568-blood vessel development | 65 | 3.66E-05 | 2.08 |
| | GO:0001944-vasculature development | 65 | 5.01E-05 | 2.03 |
| | GO:0048514-blood vessel morphogenesis | 54 | 8.71E-04 | 2.01 |
| | GO:001525-angiogenesis | 41 | 2.17E-03 | 2.17 |
| **Cluster 3 – Enrichment Score: 6.21** | | | | |
| | endoplasmic reticulum | 146 | 2.91E-08 | 1.67 |
| | GO:0005783-endoplasmic reticulum | 179 | 2.75E-05 | 1.43 |
| | GO:0044432-endoplasmic reticulum part | 64 | 6.67E-02 | 1.42 |
| **Cluster 4 – Enrichment Score: 5.12** | | | | |
| | IPR001849:Pleckstrin homology | 65 | 2.11E-03 | 1.86 |
| | domain:PH | 56 | 2.59E-03 | 1.92 |
| | SM00233:PH | 65 | 1.79E-03 | 1.76 |
| | IPR011993:Pleckstrin homology-type | 60 | 2.22E-01 | 1.57 |
| **Cluster 5 – Enrichment Score: 4.07** | | | | |
| | nucleotide binding | 278 | 5.93E-06 | 1.35 |
| | atp-binding | 226 | 8.02E-06 | 1.39 |
| | transferase | 232 | 3.14E-05 | 1.36 |
| | kinase | 129 | 3.80E-05 | 1.53 |
| | GO:0000166-nucleotide binding | 356 | 4.81E-03 | 1.24 |
| | GO:0001882-nucleoside binding | 261 | 1.56E.02 | 1.26 |
| | GO:0001883-purine nucleoside binding | 259 | 1.18E-02 | 1.26 |
| | GO:0030554-adenyl nucleotide binding | 255 | 1.05E-02 | 1.26 |
| | GO:0005524-ATP binding | 240 | 1.12E-02 | 1.27 |
| | GO:0032559-adenyl ribonucleotide binding | 242 | 1.24E-02 | 1.26 |
| | GO:0006793-phosphorus metabolic process | 165 | 2.43E-02 | 1.33 |
| | GO:0006796-phosphate metabolic process | 165 | 2.43E-02 | 1.33 |
| | GO:0004672-protein kinase activity | 111 | 1.60E-02 | 1.43 |
| | binding site: ATP | 98 | 6.76E-02 | 1.47 |
| | GO:0017076-purine nucleotide binding | 299 | 1.42E-02 | 1.21 |
| | GO:0032555-purine ribonucleotide binding | 286 | 1.72E-02 | 1.21 |
| | IPR017441:Protein kinase, ATP binding site | 85 | 1.72E-02 | 1.48 |
| | active site: proton acceptor | 113 | 2.07E-01 | 1.40 |
| | domain: Protein kinase | 84 | 1.35E-01 | 1.46 |
| | IPR000719:Protein kinase, core | 86 | 1.90E-01 | 1.43 |
| | IPR002290:Serine/threonine protein kinase | 52 | 2.30E-01 | 1.59 |
| | Nucleotide phosphate-binding region:ATP | 152 | 2.63E-01 | 1.28 |
| | serine/threonine-protein kinase | 69 | 3.41E-01 | 1.48 |
| | GO:0016310-phosphorylation | 132 | 2.82E-02 | 1.29 |
| | GO:0006468-protein amino acid phosphorylation | 112 | 1.30E-01 | 1.32 |
| | GO:0004674-protein serine/threonine kinase | 77 | 1.58E-01 | 1.39 |
| | SM00220:S_TKc | 52 | 1.15E-01 | 1.51 |
| | IPR008271: Serine/threonine protein kinase | 64 | 2.05E-01 | 1.43 |
| | IPR017442: Serine/threonine protein kinase-rela | 64 | 4.99E-01 | 1.41 |

**Table S2 – DAVID analysis of genes significantly upregulated in KD-VEGF**

| GO Cluster | Term | Count | Benjamini | Fold Enrichment |
|---|---|---|---|---|
| **Cluster 1 – Enrichment Score: 18.55** | | | | |
| | Mitochondrion | 200 | 3.39E-21 | 2.03 |
| | GO:0005739-mitochondrion | 243 | 1.36E-20 | 1.85 |
| | transit peptide | 125 | 4.79E-16 | 2.22 |
| | transit peptide: Mitochondrion | 123 | 2.66E-14 | 2.22 |
| | GO:0044429-mitochondrial part | 134 | 3.25E-11 | 1.86 |
| **Cluster 2 – Enrichment Score: 13.68** | | | | |
| | GO:0031974-membrane enclosed lumen | 352 | 2.15E-18 | 1.57 |
| | GO:0070013-intracellular organelle lumen | 339 | 4.91E-18 | 1.57 |
| | GO:0043233-organelle lumen | 342 | 2.61E-17 | 1.55 |
| | GO:0031981-nuclear lumen | 272 | 7.67E-13 | 1.55 |
| | GO:0005654-nucleoplasm | 175 | 6.55E-10 | 1.64 |
| | GO:0005730-nucleolus | 131 | 6.49E-06 | 1.55 |
| | GO:0044451-nucleoplasm part | 106 | 3.60E-05 | 1.58 |
| **Cluster 3 – Enrichment Score: 8.86** | | | | |
| | GO:0030529-ribonucleoprotein complex | 142 | 1.20E-19 | 2.28 |
| | ribonucleoprotein | 90 | 4.56E-17 | 2.73 |
| | ribosomal protein | 65 | 9.91E-14 | 2.92 |
| | GO:0006412 – translation | 95 | 3.14E-11 | 2.27 |
| | GO:0005840 – ribosome | 69 | 1.55E-12 | 2.65 |
| | GO:0033279-ribosomal subunit | 48 | 3.28E-11 | 3.10 |
| | GO:0003735-structural constituent of ribosome | 57 | 4.70E-10 | 2.76 |
| | protein biosynthesis | 48 | 1.87E-05 | 2.16 |
| | GO:0015934-large ribosomal subunit | 25 | 1.30E-05 | 3.08 |
| | hsa03010: ribosome | 30 | 3.46E-04 | 2.53 |
| | GO:0006414-translational elongation | 31 | 6.85E-04 | 2.43 |
| | GO:0022626-cystolic ribosome | 25 | 4.13E-04 | 2.55 |
| | GO:0044445–cystolic part | 37 | 9.77E-04 | 2.01 |
| | Ribosome | 22 | 1.81E-03 | 2.55 |
| | GO:0022625-cystolic large ribosomal subunit | 14 | 5.09E-03 | 3.04 |
| | GO:0022627-cystolic small ribosomal subunit | 11 | 1.71E-01 | 2.27 |
| | GO:005198-structural molecule activity | 89 | 8.50E-01 | 1.14 |
| **Cluster 4 – Enrichment Score: 8.85** | | | | |
| | GO:0000278-mitotic cell cycle | 97 | 2.15E-09 | 2.07 |
| | GO:0007049-cell cycle | 167 | 4.24E-08 | 1.65 |
| | Mitosis | 54 | 1.87E-08 | 2.50 |
| | GO:0022403-cell cycle phase | 98 | 3.96E-07 | 1.87 |
| | cell cycle | 101 | 5.33E-08 | 1.85 |
| | GO:0022402-cell cycle process | 123 | 4.49E-07 | 1.72 |
| | GO:0048285-organelle fission | 64 | 4.05E-07 | 2.21 |
| | GO:0000087-M phase of mitotic cell cycle | 62 | 1.03E-06 | 2.19 |
| | Cell division | 66 | 2.72E-07 | 2.11 |
| | GO:0000279-M phase | 80 | 2.70E-06 | 1.92 |
| | GO:0007067-mitosis | 60 | 2.91E-06 | 2.16 |
| | GO:0000280-nuclear division | 60 | 2.91E-06 | 2.16 |
| | GO:0051301-cell division | 68 | 2.25E-04 | 1.82 |

**Table S3 – DAVID analysis of genes following Expression Pattern 1**

| GO Cluster | Term | Count | Benjamini | Fold Enrichment |
|---|---|---|---|---|
| **Cluster 1 – Enrichment Score: 3.67** | | | | |
| | GO:0022402-cell cycle process | 43 | 6.85E-03 | 2.17 |
| | GO:0022403-cell cycle phase | 34 | 9.64E-03 | 2.34 |
| | GO:0000278-mitotic cell cycle | 31 | 1.19E-02 | 2.39 |
| | GO:0007049-cell cycle | 50 | 2.16E-02 | 1.84 |
| | GO:0000279-M phase | 27 | 3.91E-02 | 2.34 |
| | GO:0000087-M phase of mitotic cell cycle | 20 | 9.66E-02 | 2.55 |
| | GO:0048285-organelle fission | 20 | 1.12E-01 | 2.49 |
| | GO:0000280 nuclear division | 19 | 1.59E-01 | 2.46 |
| | GO:0007067-mitosis | 19 | 1.59E-01 | 2.46 |
| | Cell cycle | 30 | 4.49E-02 | 1.97 |
| | GO:0051301-cell division | 22 | 2.74E-01 | 2.13 |
| | cell division | 19 | 1.16E-01 | 2.18 |
| | mitosis | 15 | 1.07E-01 | 2.48 |
| **Cluster 2 – Enrichment Score: 3.10** | | | | |
| | ribonucleoprotein | 27 | 4.60E-04 | 2.93 |
| | ribosomal protein | 19 | 5.86E-03 | 3.06 |
| | GO:0005840-ribosome | 20 | 1.58E-02 | 2.75 |
| | GO:0030529-ribonucleoprotein complex | 34 | 2.37E-02 | 1.95 |
| | GO:0033279-ribosomal subunit | 14 | 2.37E-02 | 3.23 |
| | GO:0003735-structural constituent of ribosome | 16 | 4.19E-01 | 2.75 |
| | GO:0006412-translation | 23 | 3.17E-01 | 1.98 |
| | hsa03010:Ribosome | 8 | 9.95E-01 | 2.24 |
| | GO:0005198-structural molecule activity | 23 | 9.94E-01 | 1.05 |
| **Cluster 3 – Enrichment Score: 2.61** | | | | |
| | GO:0005739-mitochondrion | 65 | 2.75E-03 | 1.77 |
| | GO:0044429-mitochondrial part | 42 | 2.08E-03 | 2.08 |
| | Mitochondrion | 48 | 1.79E-02 | 1.74 |
| | Transit peptide: mitochondrion | 30 | 7.81E-01 | 1.93 |
| | GO:0031090-organelle membrane | 57 | 5.12E-02 | 1.54 |
| | Transit peptide | 30 | 5.81E-02 | 1.91 |
| | GO:0031966-mitochondrial membrane | 25 | 1.07E-01 | 1.87 |
| | GO:0005740-mitochondrial envelope | 26 | 1.01E-01 | 1.83 |
| | GO:0031980-mitochondrial lumen | 17 | 9.89E-02 | 2.21 |
| | GO:0005759-mitochondrial matrix | 17 | 9.89E-02 | 2.21 |
| | GO:0031967-organelle envelope | 33 | 1.68E-01 | 1.57 |
| | GO:0031975-envelope | 33 | 1.67E-01 | 1.57 |
| | GO:0005743-mitochondrial inner membrane | 17 | 4.22E-01 | 1.64 |
| | GO:0019866-organelle inner membrane | 17 | 5.50E-01 | 1.53 |
| | Mitochondrion inner membrane | 11 | 6.46E-01 | 1.72 |
| **Cluster 4 – Enrichment Score: 2.34** | | | | |
| | GO:0051726-regulation of cell cycle | 26 | 8.71E-02 | 2.24 |
| | GO:0010564-regulation of cell cycle process | 12 | 2.96E-01 | 3.00 |
| | GO:0007346-regulation of mitotic cell cycle | 14 | 3.29E-01 | 2.63 |
| | GO:0007093-mitotic cell cycle checkpoint | 7 | 3.48E-01 | 4.65 |
| | GO:0000075-cell cycle checkpoint | 9 | 5.34E-01 | 2.82 |
| | GO:0031575-G1/S transition checkpoint | 3 | 9.15E-01 | 5.04 |
| **Cluster 5 – Enrichment Score: 2.32** | | | | |
| | GO:0005761-mitochondrial ribosome | 8 | 5.48E-02 | 4.92 |
| | GO:0000313-organellar ribosome | 8 | 5.48E-02 | 4.92 |
| | GO:0005763-mitochodrial small ribosomal | 4 | 2.35E-01 | 6.56 |

| | | | |
|---|---|---|---|
| GO:0000314-organellar small ribosomal | 4 | 2.35E-01 | 6.56 |

**Table S4 – DAVID analysis of genes following Expression Pattern 2**

| GO Cluster | Term | Count | Benjamini | Fold Enrichment |
|---|---|---|---|---|
| **Cluster 1 – Enrichment Score: 5.70** | | | | |
| | GO:0048514-blood vessel morphogenesis | 23 | 1.00E-03 | 3.60 |
| | GO:0001568-blood vessel development | 24 | 1.75E-03 | 3.23 |
| | GO:0001944-vasculature development | 24 | 1.77E-03 | 3.15 |
| | GO:0001525-angiogenesis | 17 | 5.94E-03 | 3.79 |
| **Cluster 2 – Enrichment Score: 4.33** | | | | |
| | GO:0016477-cell migration | 24 | 5.16E-03 | 2.87 |
| | GO:0048870-cell motility | 24 | 2.30E-02 | 2.58 |
| | GO:0051674-localization of cell | 24 | 2.30E-02 | 2.58 |
| | GO:0006928-cell motion | 31 | 3.71E-02 | 2.15 |
| **Cluster 3 – Enrichment Score: 2.23** | | | | |
| | hsa04360:Axon guidance | 14 | 1.13E-01 | 2.94 |
| | domain: Sema | 6 | 5.97E-01 | 6.50 |
| | IPR002165: Plexin | 6 | 6.38E-01 | 6.36 |
| | IPR001627:Semaphorin/CD100 antigen | 6 | 6.38E-01 | 6.36 |
| | IPR003659: Plexin/semaphorin/integrin | 7 | 4.97E-01 | 5.11 |
| | SM00630:Sema | 6 | 5.93E-01 | 5.60 |
| | SM00423:PSI | 7 | 3.89E-01 | 4.50 |
| | IPR015943:WD40/YVTN repeat-like | 15 | 9.47E-01 | 1.64 |
| | Domain:Ig-like C2-type | 5 | 1.00E+00 | 1.63 |
| **Cluster 4 – Enrichment Score: 1.83** | | | | |
| | IPR013761:Sterile alpha motif-type | 10 | 3.81E-01 | 4.27 |
| | IPR001660:Sterile alpha motif-SAM | 9 | 8.11E-01 | 3.18 |
| | SM00454:SAM | 9 | 6.85E-01 | 2.80 |
| | domain:SAM | 7 | 9.59E-01 | 2.90 |
| | IPR011510:Sterile alpha motif homology 2 | 3 | 9.98E-01 | 2.40 |
| **Cluster 5 – Enrichment Score: 1.74** | | | | |
| | GO:0030054-cell junction | 26 | 7.19E-01 | 1.67 |
| | cell junction | 21 | 3.46E-01 | 1.78 |
| | GO:0005911-cell-cell junction | 12 | 6.30E-01 | 2.10 |
| **Cluster 6 – Enrichment Score: 1.73** | | | | |
| | actin-binding | 16 | 2.07E-01 | 2.19 |
| | GO:0008092-cytoskeletal protein binding | 26 | 7.74E-01 | 1.67 |
| | GO:0015629-actin cytoskeleton | 16 | 6.39E-01 | 1.97 |
| | GO:0003779-actin binding | 16 | 9.44E-01 | 1.59 |
| **Cluster 7 – Enrichment Score: 1.63** | | | | |
| | GO:0001667-ameboidal cell migration | 6 | 6.73E-01 | 5.35 |
| | GO:0014032-neural crest cell development | 5 | 7.91E-01 | 5.00 |
| | GO:0014033-neural crest cell differentiation | 5 | 7.91E-01 | 5.00 |
| | GO:0060485-mesenchyme development | 6 | 8.10E-01 | 3.81 |
| | GO:0001755 neural crest cell migration | 4 | 8.08E-01 | 5.74 |
| | GO:0014031-mesenchymal cell development | 5 | 8.54E-01 | 3.23 |
| | GO:0048762-mesenchymal cell differentiation | 5 | 8.54E-01 | 3.23 |